

Using multi-angle, multispectral photo-polarimetry of the NASA Glory mission to constrain optical properties of aerosols and clouds: Results from four field experiments

Jacek Chowdhary^a, Brian Cairns^a, Michael I. Mishchenko^b, Larry D. Travis^b

^aDept. of Appl. Phys. and Appl. Math., Columbia University, 2880 Broadway, New York, NY USA

^bNASA/Goddard Institute for Space Studies, 2880 Broadway, New York, NY USA

ABSTRACT

Tropospheric aerosols play a crucial role in climate and can cause a climate forcing directly by absorbing and reflecting sunlight, thereby cooling or heating the atmosphere, and indirectly by modifying cloud properties. The indirect aerosol effect may include increased cloud brightness, as aerosols lead to a larger number of smaller cloud droplets (the so-called Twomey effect), and increased cloud cover, as smaller droplets inhibit rainfall and increase cloud lifetime. Both forcings are poorly understood and may represent the largest source of uncertainty about future climate change. In this paper we present results from various field experiments demonstrating the contribution that the multi-angle multi-spectral photopolarimetric remote sensing measurements of the NASA Glory mission will make to the determination of the direct and indirect radiative effects of aerosols.

Keywords: Photometry, polarimetry, aerosol, cloud, indirect effect

1. INTRODUCTION

Aerosols can change the radiative budget of the atmosphere by scattering or absorbing sunlight (“direct climate forcing”) and by modifying the formation and life-cycle of clouds (“indirect climate forcing”). Radiative balance computations suggest that the sum of these forcings can be comparable to that of anthropogenic greenhouse gasses; however, the magnitude and even sign of this sum remains one of the largest unknown factors in climate research¹. Aerosols also pose a problem in retrieving properties of the ocean from space-borne observations (“atmospheric correction”). For example, radiative transfer simulations show that a small uncertainty in this contribution can lead to large errors in the retrieval of Chlorophyll *a* concentrations in the ocean². To constrain the aerosol climate forcings requires accurate characterizations of the particle size, complex refractive index, and number density of aerosol and cloud particles on a global scale – i.e., from satellite observations³. These characterizations will also clearly benefit the remote sensing retrieval accuracy of Chlorophyll *a* concentrations in the ocean. In this work, we discuss the unique capabilities of remote sensing polarimetry to provide such characterizations.

The NASA Glory mission⁴ which is planned to launch in 2008 will carry an Aerosol Polarimeter Sensor (APS) for the determination of aerosol and cloud properties and a Total Irradiance Monitor (TIM) instrument to monitor the changes in total solar irradiance (TSI) incident on the atmosphere of the Earth. The Glory spacecraft will also carry two simple cloud cameras operating each at 412 and 865 nm that will be used to determine the amount of cloud that is occurring within the APS instantaneous field of view (IFOV) instrument. The APS sensor will provide high-precision measurements of the total and polarized reflectance in 9 narrow spectral bands ranging from 412 to 2250 nm, and in 240 viewing angles with the scan oriented along the spacecraft ground track covering an angular range of 60° from nadir on one side of the scan and to the limb of the Earth on the other side. It therefore combines the spectral coverage of the MODerate resolution Imaging Spectrometer (MODIS) instrument, the multiangle views of the Multiangle Imaging Spectro-Radiometer (MISR) instrument, and the polarization measurements of the POLarization and Directionality of Earth Reflectances (POLDER) instrument to obtain the most complete set of information available on the solar radiation reflected by the Earth’s system in the visible (VIS) and near-infrared (NIR) part of the spectrum.

The need for such extensive sets of data to retrieve aerosol properties becomes clear when considering the ambiguities that arise in such retrievals when using only MODIS-like, MISR-like, or POLDER-like data sets⁵. These ambiguities arise because of the assumptions that have to be made about the composition and size of aerosol particles

prior to the inversion of such data subsets. Similar assumptions are required for the retrieval of extinction to backscatter ratio from elastic backscatter lidar measurements. Data obtained by the Research Scanning Polarimeter (RSP) instrument⁶, which provides a similar capability to the APS, show that many of these assumptions can be eliminated by the information content of multiangle, multispectral total *and* polarized reflectances, such that it is possible to retrieve the optical depth, single scattering albedo, refractive index, and size distribution of a bimodal aerosol from these reflectances. Moreover, polarimetric remote sensing provides this capability over both land and water surfaces, and for observations in the visible part of the spectrum.

Retrieving the microphysical properties of clouds from passive remote sensing of their total reflectance also requires prior knowledge: of the effective variance of their droplet size distribution in the case of water clouds and of the shape distribution of the crystals in the case of ice clouds. Polarized reflectances on the other hand are not only sensitive to the effective radius but also to the effective variance of cloud droplets, and allow a plausible particle shape distribution to be estimated in the case of ice clouds. Furthermore, for water clouds a plausible vertical profile of droplet size can be retrieved because of the significantly different vertical weighting profiles of total and polarized reflectance measurements. Finally, they allow the cloud top and cloud base pressure to be determined which allows the physical thickness of a cloud to be estimated. This in turn allows us to estimate the number concentration of droplet or ice particles in clouds which is the crucial parameter needed in evaluating the indirect effect of aerosols on clouds.

We demonstrate some of these capabilities to retrieve aerosol and cloud properties using RSP measurements taken during the Chesapeake Lighthouse and Aircraft Measurements for Satellites (CLAMS), the Cirrus Regional Study of Tropical Anvils and Cirrus Layers – Florida Area Cirrus Experiment (CRYSTAL-FACE), the Coastal STRatocumulus Imposed Perturbation Experiment (CSTRIPE) and using RSP measurements taken over smoke aerosols in Southern California. In some of these experiments vignetting by the skin of the aircraft limits the angles that are available for each scan and only view angles that are clearly free from any vignetting are used in the analyses that follow. The scan plane can be oriented either along the along the ground track of the aircraft to sample multiple views of the same scene, or perpendicular to this plane to obtain maximum areal coverage. All of the data analyzed here has the RSP oriented along the aircraft ground track. The total reflectance R and polarized reflectance P analyzed in this study are defined as $\pi I (\mu_0 S)^{-1}$ and $\pi(Q^2+U^2)^{1/2} (\mu_0 S)^{-1}$, respectively, where μ_0 is the cosine of the solar zenith angle θ_0 ($^\circ$) and S is the modified extraterrestrial solar irradiance ($\text{W m}^{-2} \text{nm}^{-1}$). The latter irradiance is the RSP instrument spectral response convolved with the solar spectral irradiance.

2. THE AEROSOL POLARIMETRY SENSOR

Although the data that we analyze in this paper was taken with the RSP instrument, here we will briefly describe the design of the APS and how it is expected to produce measurements of similar, or better quality, to the RSP when on orbit. The APS instrument is similar to the RSP instrument⁶ in that it allows the total and linearly polarized reflectance to be measured simultaneously in nine spectral channels for each instantaneous field of view (IFOV). This is accomplished by six boresighted telescopes that have the same IFOV of 8 mrad. The refractive telescopes are paired, with each pair making measurements in three spectral bands. One telescope in each pair makes simultaneous measurements of the linear polarization components of the intensity in orthogonal planes at 0° and 90° to the meridional plane of the instrument (using Wollaston prisms to spatially separate the orthogonal polarizations onto a pairs of detectors), while the other telescope in a pair simultaneously measures equivalent intensities in orthogonal planes at 45° and 135° . These measurements provide the simultaneous determination of the Stokes parameters I , Q , and U in nine spectral bands with a wide dynamic range (16-bit digitization) and high signal-to-noise ratio (greater than 250 at radiance levels typical of aerosols over the ocean) with a radiometric and polarimetric uncertainty of $\leq 5\%$ and $\leq 0.2\%$, respectively. This measurement approach ensures that the polarization signal is not contaminated by scene intensity variations during the course of the polarization measurements, which could create “false” or “scene” polarization.

The APS spectral bands are divided into two groups based on the type of detector used: visible/near infrared (VNIR) bands using UV-enhanced silicon photodiodes at wavelengths of 412 (20), 443 (20), 555 (20), 672 (20), 865 (39) and 910 (20) nm and short-wave infrared (SWIR) bands using HgCdTe photodiodes (cooled to 163K) at wavelengths of 1378 (35), 1610 (60), and 2250 (75) nm. Dichroic beam splitters are used for spectral selection, while interference filters define the spectral bandpasses of each band. The parenthetic figures are the full width at half maximum (FWHM) bandwidths of the spectral bands. These spectral bands are capable of sampling most of the spectral variations in reflected sunlight due to particle scattering in the atmosphere. That is, the 412-, 443-, and 555-nm reflectances are significantly affected by molecular scattering in addition to scattering by sub-micron and super-micron

(including cloud) particles. The 672- and 865-nm reflectances on the other hand are predominantly caused by scattering due to sub-micron and super-micron particles, and the 1590-, 1880-, and 2250-nm reflectances by scattering due to super-micron particles only. The 910- and 1378-nm bands are further sensitive to the amount of water vapor and to the presence of cirrus clouds, respectively. The 8 mrad IFOV's are continuously scanned by a polarization-neutral two-mirror system which allows 240 viewing-angle samples (with a dwell time of 1.9 msec for each sample) to be acquired over a 112.5° angular range (+50°, -62.5° about nadir) as measured at the spacecraft swath. At the expected orbital altitude of 824 km this will provide a view zenith angle range at the surface of the earth of +60° to limb about nadir with a nadir pixel size of 6.6 km.

The primary difference between the spaceflight APS and the aircraft based RSP is that the APS must provide a complete set of in-flight calibration measurements that allow the radiometric and polarimetric accuracy to be maintained over the course of the mission. The APS will have four calibration references. 1) A dark cavity provides reference dark measurements for each APS scan which defines the zero radiance level extremely accurately. 2) A solar reference to define the radiometric scale and provide the calibration coefficients linking counts to observed radiance levels. 3) An unpolarized reference to determine relative gain coefficients of detectors measuring orthogonal polarizations. 4) A polarized reference to identify and correct for any contamination induced cross-talk, or depolarization.

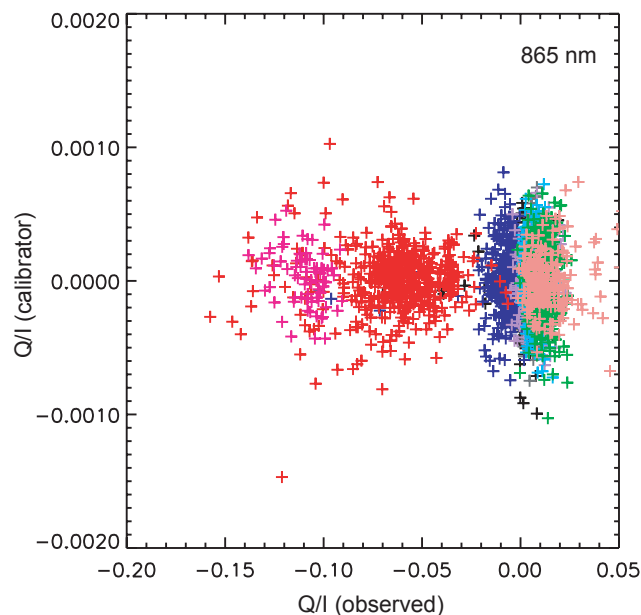


Fig. 1. Output from unpolarized reference as a function of input polarization for single measurements over clouds during CSTRIFE.

The solar reference has a cover that is a one-time deployable and will be made of Spectralon. It is expected that the reflectance of this reference will decrease over the course of its life, particularly in the UV and it will be used to define the radiometric scale at the time of initial deployment of its cover. Subsequently the radiometric stability of the APS will be tracked using lunar observations⁷. The unpolarized reference will use a polarization scrambler⁸ to create scenes of very low polarization. The efficacy of this approach has been demonstrated by the RSP instrument as shown in Fig. 1 where it can be seen that the polarization provided by the unpolarized reference is very low (< 0.1%) over a wide range of input polarization states. The scatter in these measurements is caused by the noise present in a single measurement and by averaging we find that the

mean polarization provided by the unpolarized reference is 0.02%. This reference will be observed on every scan, but it is expected that any small changes in the relative gain coefficients that are determined from this reference will be sufficiently small that data from an entire orbit will be used in this process. The polarized reference will use crystalline polarizers to create scenes with very high polarization. This reference will also be observed on every scan and similarly to the unpolarized reference it is expected that any changes to the calibration coefficients determined using this reference will change no faster than an orbital period. We should note that our experience with the RSP instrument is that the calibration coefficients determined with the unpolarized and polarized reference change on a time-scale of years even when operated in the hostile environment of a small survey plane (vibration, coated with oil etc.).

3. THE CLAMS FIELD EXPERIMENT

3.1 Description and objectives

The Chesapeake Lighthouse and Aircraft Measurements for Satellites (CLAMS) experiment, which took place during the period of July 10 to August 2, 2001, offers a unique opportunity to explore how well remote sensing measurements, such as those made by the RSP, can constrain the properties of aerosol particles over the ocean. The CLAMS experiment was a short-wave radiative closure experiment that involved measurements obtained from six research aircraft, several land sites, and an ocean platform. Its goal was to validate and improve atmospheric and

oceanic products retrieved from observations by the CERES (Clouds and Earth's Radiant Energy System), the MISR, and the MODIS satellite instrument flown onboard the Earth Observing System (EOS) spacecraft Terra. The majority of the measurements were centered close to the Chesapeake Lighthouse research platform, which is located 25 km east of Virginia Beach and which functions as the CERES Ocean Validation Experiment (COVE) site where radiation, meteorology, and ocean optics are monitored continuously.

The RSP instrument participated in the CLAMS experiment from 10 July to 17 July 2001. More than 150 files of flight track data were acquired during this period over ocean near the COVE site and over land crossing the Dismal Swamp (available at http://www.giss.nasa.gov/data/rsp_air/clamsindex.html). RSP data were acquired at high (3.6 km) and low (60 m) altitudes. The low altitude measurements were designed to meet the desire of the CERES, MODIS and MISR teams for better characterization of the surface bidirectional reflectance distribution function (BRDF) and the high altitude measurements were designed to study the retrieval of aerosol properties from satellite observations. Other components of the CLAMS experiment that are of interest in this work are the in situ measurements of aerosol scattering and absorption coefficients and aerosol extinction optical depths collected by the instruments aboard the University of Washington Convair-580 research aircraft^{9,10}, the ocean optics measurements performed from the COVE ocean platform¹¹ and the optical depth measurements made by AERONET¹².

3.2 RSP retrievals

The approach commonly followed in remote sensing of aerosols over the ocean occurs in two steps^{13,14}. The first step consists of identifying a predefined aerosol model and estimating its optical depth such that a best fit is obtained to measurements of the total reflectance in the NIR, where one can ignore the contribution of waterleaving reflectances. The second step consists of extrapolating the aerosol optical properties from the NIR to the VIS to either retrieve the waterleaving reflectances or to estimate the magnitude of direct climate forcing. The difficulty of this approach is that the NIR selection of an aerosol model suffers from serious nonuniqueness problems if it is based on total reflectance measurements, that the extrapolation to the VIS requires the spectral variation of the aerosol refractive index to be assumed, and that the retrieval of aerosol single scattering albedo is accomplished best from total reflectance measurements in the VIS rather than in the NIR. The polarized reflectances obtained by the RSP instrument in the NIR are, on the other hand, very sensitive to the aerosol size distribution and real refractive index⁵. Furthermore, the contribution in the VIS to these reflectances of underwater light scattering can be ignored for a wide range of viewing angles around the backscattering direction in the principal and estimated quite nicely for the other scattering geometries¹⁵. This allows for the retrieval of aerosol real refractive indices from the polarized reflectances obtained by the RSP instrument to be continued in the VIS. It also causes the retrievals of aerosol single scattering albedo and ocean color from total reflectances in the VIS to be much more accurate.

To illustrate some of these points, we analyze RSP data acquired near the Chesapeake Lighthouse platform during the CLAMS campaign on July 17th, 2001. To constrain the properties of aerosols that are close in space and time to measurements of the sky- and underwater-light performed from the Chesapeake Lighthouse platform, we use the data collected during RSP flight 027. The ground track for this flight grazed the COVE site between 1616 to 1618 UTC, which encompasses the aerosol optical depth measurements by AERONET at 1617 UTC and is closest to the site of ocean optics measurements obtained at 1605 UTC. It crosses further the ground track of Convair-580 flight 1874 a few minutes ahead of time. The cruising height of RSP flight 027 was 3.6 km, and the RSP scan plane was oriented in the solar principal plane during this flight. The solar zenith angle for this flight was about 19°. To minimize the effect of spatial variations, we analyze the average of 100 consecutive scans closest to the COVE site. The error bars in Fig. 2 show the standard deviation of total (first row) and polarized (second row) reflectances obtained by the RSP instrument at 410 nm. The solid line shows the fit for the RSP retrieved fine-mode aerosol. The size distribution for this aerosol is characterized by an effective radius $r_e = 0.15 \mu\text{m}$ and effective variance $v_e = 0.2$, and its refractive index m by the real part $\text{Re}[m] = 1.46$ and imaginary part $\text{Im}[m] = 0.01$. Note that we include the contribution of waterleaving reflectances derived from ocean color (OC) in situ data. The broken lines in the first, second, and third columns show the results for changes in $\text{Re}[m]$, in $\text{Im}[m]$, and in the waterleaving radiances. The aerosol optical thickness τ for the perturbation cases in the first two columns was changed to fit the total reflectance measurements at 865 nm, where the contribution of waterleaving reflectances can be ignored for open ocean observations. We observe first that the polarized reflectances are highly sensitive to $\text{Re}[m]$ and nearly insensitive to waterleaving radiances for these scattering geometries, while the opposite is true for the total reflectances. Secondly, both reflectances are sensitive to $\text{Im}[m]$ for this aerosol size distribution. Hence, the retrieval of $\text{Im}[m]$ depends on the estimate of the ocean color for total reflectance inversions and on the $\text{Re}[m]$ estimate for polarized reflectance inversions. However, the $\text{Re}[m]$ and $\text{Im}[m]$ retrievals can further be constrained by limiting their spectral variations while there are less

constrains available for the ocean color estimate. We remark that the fine-mode aerosol products resulting from this RSP case study were in excellent agreement with in situ and sky-light measurements¹⁶.

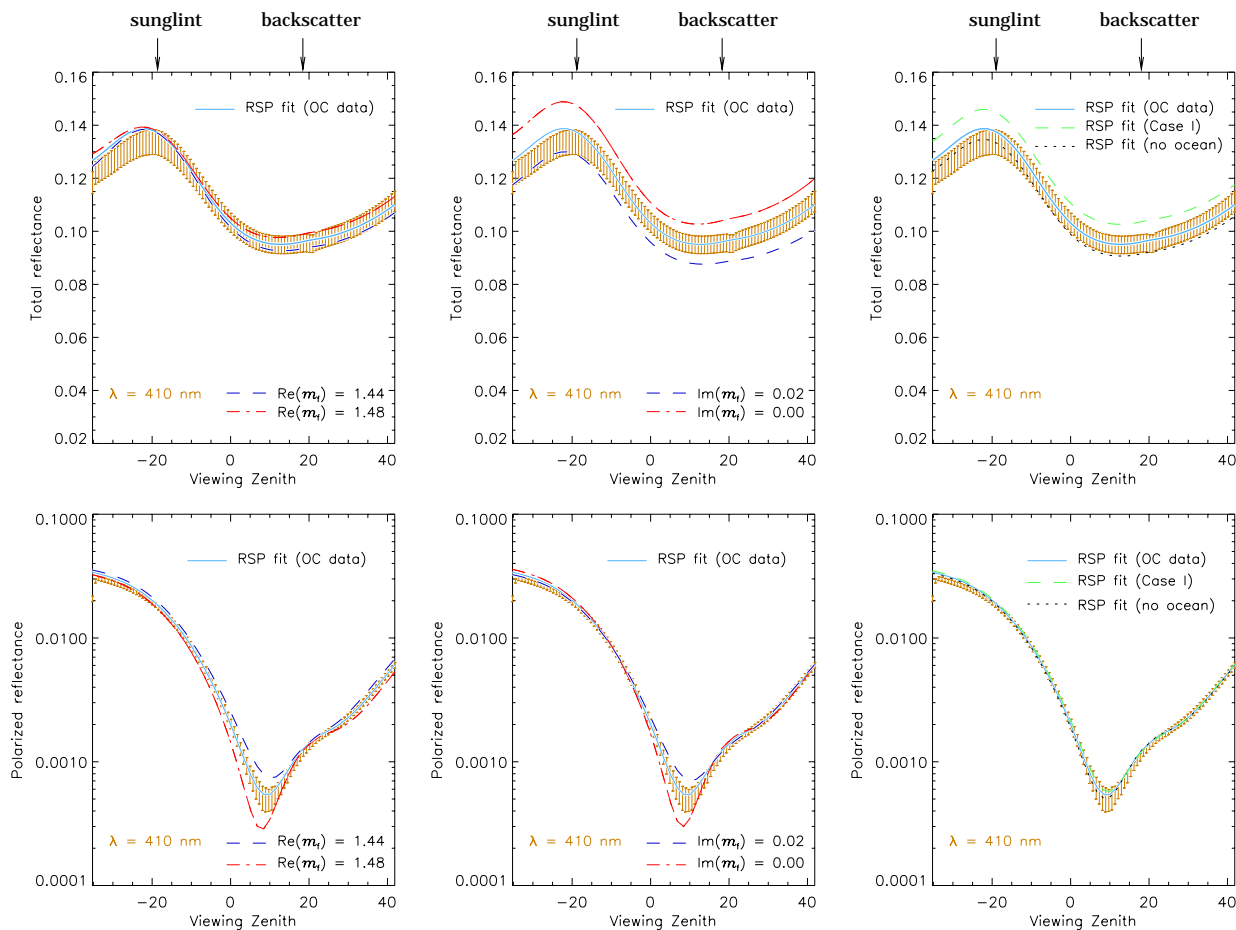


Fig. 2. Analyses of the sensitivity of RSP data to variations in the aerosol refractive index m and the ocean color OC. The error bars denote the combined standard deviation of total reflectance (first row) and polarized reflectance (second row) measured by the RSP instrument at $\lambda = 410$ nm. The solid curve is the fit for the RSP retrieved fine aerosol and includes the ocean color contribution derived from in situ data. The broken curves are the numerical results for changes in $\text{Re}[m]$ by ± 0.02 (first column), for changes in $\text{Im}[m]$ by ± 0.01 (second column), and for ignoring and including waterleaving radiances derived from a bio-optical model for a Case I (open ocean) water with $[\text{Chl}] = 1 \text{ mg/m}^3$ (third column).

4. THE CRYSTAL-FACE FIELD EXPERIMENT

4.1 Description and objectives

CRYSTAL-FACE is a measurement campaign that took place during the month of July, 2002, over southern Florida and the surrounding waters where deep convection is known to occur frequently in this month. Its primary goal was to investigate the formation and evolution of tropical cirrus anvils as well as their cloud physical properties on a case by case study approach. Six aircrafts were involved in obtaining remote sensing data and in situ measurements of aerosols, ice crystals, meteorological fields, radiative fluxes, and gas concentrations. In addition, ground-based measurements were collected by multi-frequency millimeter radar, lidar, and radiometry instruments located in southwestern and southeastern Florida. Data collected during the CRYSTAL-FACE campaign will also play a crucial role in validating cloud property retrievals employed for current spaceborne missions such as Terra, Aqua and the Tropical Rainfall Measuring Mission (TRMM), and for developing cloud inversion algorithms for future missions such as the Cloud-Aerosol Lidar and Infrared Pathfinder Satellite Observation (CALIPSO), CloudSat, and EOS-Aura.

The RSP instrument participated in the CRYSTAL-FACE campaign onboard a Proteus aircraft in support of the National Polar-orbiting Environmental Satellite System (NPOESS) mission, which is a joint enterprise by NASA, the Department of Defense (DoD), and the Department of Energy (DoE). The Proteus aircraft flew 12 successful flights in the lower stratosphere, all of during which the RSP instrument collected 130 files of flight track data both over land and ocean surfaces (available at <ftp://crystal-face.giss.nasa.gov>). Other airborne data of interest to the analyses of RSP reflectances are the meteorological records and in situ measurements of aerosol and cloud particle properties collected by the NASA WB-57 aircraft in the tropopause region, by the Cessna Citation II aircraft of the University of North Dakota in the mid- to upper-troposphere, and by the UV-18A aircraft of the Naval Postgraduate School in Monterey (CA) in the boundary region.

4.2 RSP retrievals

Although there have so far been limited attempts to evaluate the effect of aerosols on ice clouds recent results suggests aerosols may play a significant role in determining ice particle sizes¹⁷ and consequently in determining precipitation rates. It will therefore become more important in the future to have accurate global estimates of ice particle sizes. A common problem in the current remote sensing of ice clouds is that the shape of the crystals is unknown and any errors in the assumed shape can propagate into errors in the estimated particle size and optical depth¹⁸. The multi-angle measurements made by the APS sensor can reduce these biases since the measurements allow a plausible shape distribution of particles to be determined. An example is shown in Fig. 3 where multi-angle polarized reflectance measurements are compared against several shape distributions. Only a shape distribution that included small (5 μm) spheroids was acceptable for this cold cloud (200K) case and this assignment was borne out by in situ size distribution measurements and images from a cloud particle imager. The estimated optical depth of this thin cirrus cloud (0.1) is also in agreement with Cloud Polarization Lidar (CPL) measurements indicating the capability of the planned APS polarimetric measurements to identify particle shape and derive realistic cloud ice particle sizes and optical depths.

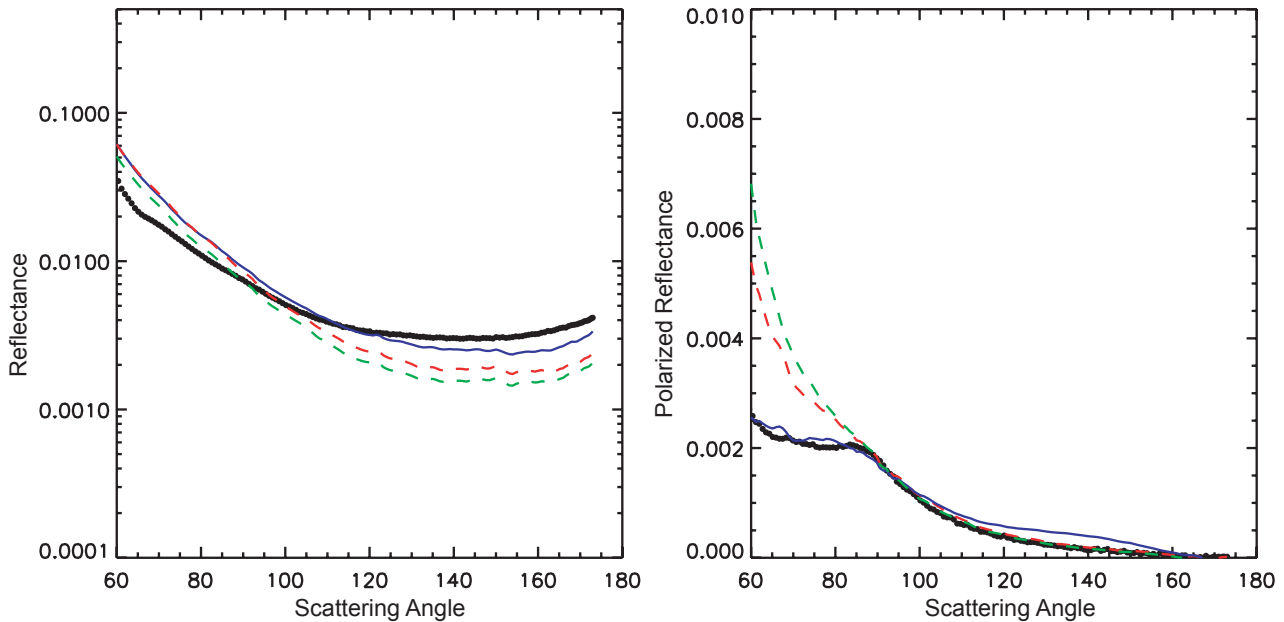


Fig. 3. Fits between measurements (black) of reflectance and polarized reflectance at 1880 nm using the RSP and calculations using an optical depth of 0.1 for i) 50 μm effective radius fractal polycrystals (dashed red line) ii) 25% 5 μm spheroids mixed with the fractal polycrystals (blue line) and iii) 25% hexagonal plates mixed with the fractal polycrystals (green line).

These measurements are of interest to a global understanding of clouds since existing size and shape distribution measurements tend to be biased towards warmer mid-latitude cirrus clouds than the example presented here. These cold sub-tropical clouds appear to have smaller particles¹⁹ and have significant quantities of spheroidal particles and small irregular particles which are not assumed to be present in current retrieval methods¹⁸. Since these small particles may be affected by pollution in unexpected ways¹⁷ and can have a noticeable effect on the radiative properties of cirrus clouds¹⁹ it would appear that the capability to measure them is of considerable value in determining the effect of

aerosols on clouds. Furthermore, the asymmetry parameters of these small particle (0.81-0.83; *Liu et al.*²⁰) may be larger than that for the larger particles (0.75) that have been observed in warmer cirrus clouds¹⁹ with consequent differences for the radiative effects of the small particles. Measurements of the asymmetry parameter for the coldest clouds have never been successfully made and it has simply been assumed that the temperature independent behavior of the asymmetry parameter observed for warmer cirrus clouds will persist for the colder clouds with very small ice crystals. Since the mechanisms that appear to be responsible for the low asymmetry parameters of large particles are roughness and inclusions^{21,22}, it is not clear that this assumption will be valid for the small ice crystal observed in the coldest thin cirrus clouds because of their formation process and the low likelihood of collisions with other crystals that could cause roughening, or damage.

5. THE CSTRIFE FIELD EXPERIMENT

5.1 Description and objectives

The Coastal STRatocumulus Imposed Perturbation Experiment (CSTRIFE) was a field campaign organized by the California Institute of Technology, the Center for Interdisciplinary Remotely-Piloted Aircraft Studies (CIRPAS), the Naval Postgraduate School, the University of Miami, and the National Center for Atmospheric Research (NCAR) to study the effect of aerosols on the microphysics, precipitation and dynamics of marine stratocumulus clouds. The campaign was conducted in a three-week mission off the coast of Monterey, California in July, 2003, and used instruments onboard the CIRPAS Twin Otter aircraft to perform closure as well as perturbation studies on aerosol-cloud-radiation interactions. Samples were acquired of local fire plumes, polluted air masses, unperturbed marine stratocumulus clouds, and stratocumulus clouds perturbed by seeding flares.

During five days of this campaign, a separate aircraft carrying the RSP instrument overflew the Twin Otter to and collected almost 120 files of reflectance data (available at <ftp://crystal-face.giss.nasa.gov>) to provide remote sensing information on aerosol particles, of cloud condensation nuclei, and of cloud particles. This information can directly be compared with data collected by a number of instruments onboard the Twin Otter aircraft which include three aerosol sizing probes, a CCN spectrometer; an aerosol mass spectrometer, three light absorption instruments, three cloud microphysics probes, a multi-channel radiometer, and upward and downward facing pyranometers including a stabilized platform for reliable measurements of albedo.

5.2 RSP retrievals

In determining the effect of aerosols on clouds it is essential that the cloud properties that are used do not have biases that depend on the type of cloud, or season. Existing methods for remotely determining the size of cloud droplets use the fact that the efficiency of liquid and ice absorption depends on particle size^{23,24}, or that the rainbow and glory features of radiation scattered by spherical particles are sensitive to particle size^{25,26}. Methods using the efficiency of liquid and ice absorption must assume an effective variance of the droplet size distribution in their retrievals, which can cause biases in the estimated effective radius if incorrect²³. Existing analyses of the rainbow and glory features in the radiation scattered by liquid water droplets are limited to very narrow size distribution widths for which these features have a large magnitude: This may cause sampling biases that seriously affect evaluations of aerosol-cloud interactions.

The APS sensor makes measurements that allow both methods to be combined and reduces their limitations. Polarized reflectance measurements are sensitive to the droplet size distribution (effective radius and effective variance) in the top layer of the cloud (optical depth less than three) while the reflectance measurements in spectral bands where ice and water absorb (1.6 and 2.25 μm) are sensitive to a weighted integral through the depth of the cloud²⁷. The type of measurements made by APS therefore require a cloud model with two vertical layers. This allows the complete set of measurements to be matched with the additional benefit of providing sensitivity to the vertical profile of droplet size and consequently reducing any biases in the estimated liquid water path and number density of droplets. In addition the polarized reflectance at scattering angles well separated from the rainbow and glory can be used to determine cloud top height²⁵ and the optical properties of haze above cloud top. An example of the fit that can be obtained between model and measurements at a pair of wavelengths (0.865 and 2.25 μm) is shown in Fig. 4.

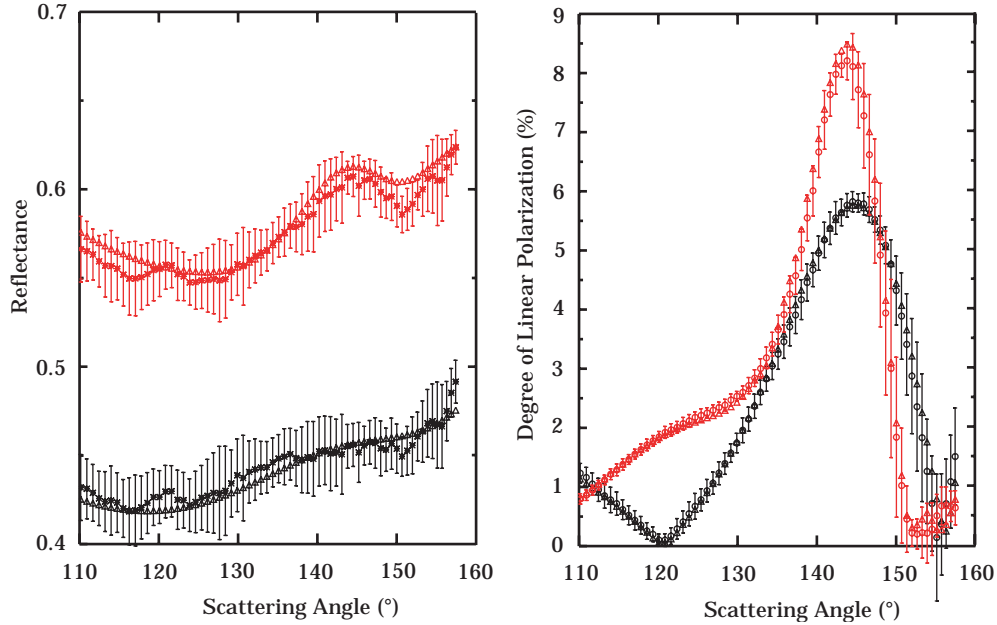


Fig. 4. Comparison of model calculations (triangular symbols) and measurements (circular symbols with error bars) of reflectance and degree of linear polarization at 0.865 and 2.25 μm for a best fit two layer cloud model. Measurements were obtained with the RSP with a pixel size of 40 m. Analysis is for a ten pixel average and the error bars are primarily a result of cloud variability over this 400 m strip.

The retrieved properties at cloud top and for a weighted integral through the cloud that is consistent with size retrievals using the 2250 nm reflectance measurements are compared with in situ particle size measurements from an FSSP instrument in Table 1.

Table 1. Comparison between remotely sensed and in situ determinations of cloud droplet effective radius r_e and effective variance v_e . A) Cloud top retrieval compared with polarized reflectance retrieval. B) Weighted integral compared with reflectance retrieval.

property	7/22/2003			7/25/2003		
	r_e (A)	v_e (A)	r_e (B)	r_e (A)	v_e (A)	r_e (B)
RSP retrieval	7.938	0.039	7.105	9.228	0.152	8.985
FSSP retrieval	8.726	0.067	8.01	9.365	0.176	8.69

It is clear that not only is the cloud droplet effective radius accurately estimated, but also the effective variance of the droplet size distribution. Although the effective variance is a secondary variable in determining the radiative properties of clouds it is necessary to have accurate estimates of the effective variance in order to determine the concentration of cloud drops which is a key diagnostic of the indirect effect of aerosols on clouds^{3,28}. The effective variance of the cloud droplet size distribution is also a diagnostic measure of the relative contributions of dynamics, thermodynamics and aerosols to the cloud formation process^{29,30}.

6. SOUTHERN CALIFORNIA SMOKE MEASUREMENTS

6.1 Description and objectives

Several massive wildfires were raging across southern California over the weekend of October 25, 2003. Whipped by the hot, dry Santa Ana winds that blow toward the coast from interior deserts, at least one fire grew 10,000 acres in just 6 hours. The fires continued to burn over the next week and on the 29th October we installed the RSP instrument on a small survey plane (Cessna 210) and flew over some of the fires in the Simi Valley area and over the Mojave Desert to where a significant amount of smoke had been transported. The aim of this flight was to try and characterize

the microphysical properties of the aerosol and in particular to try and obtain estimates of the real refractive index of the smoke aerosols in this very dry environment.

6.2 RSP retrievals

In analyzing polarimetric measurements over land we have found that the surface polarized reflectance is typically grey. This greatly simplifies the process of performing aerosol retrievals over land using polarization measurements since the longest wavelength measurement, which is least affected by aerosols, can then be used as a proxy for the surface at all shorter wavelengths as a first guess. The aerosol model that is retrieved can then be used to correct the longest wavelength measurements for the effects of aerosol and obtain an improved estimate of the surface polarized reflectance.

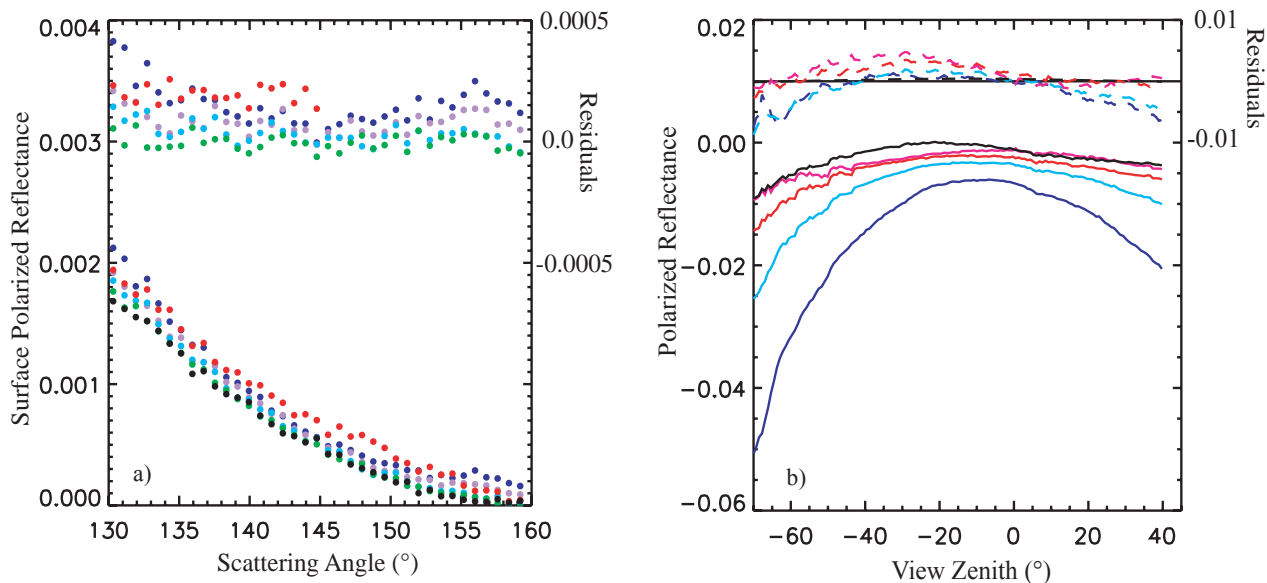


Fig. 5 a) Surface polarized reflectance at 410, 470, 555, 673, 865 and 2250 nm (blue, mauve, turquoise, green, red and black) with the difference between the 2250 nm observations and the other bands being shown as residuals. b) Observed polarized reflectance at an altitude of 3500 m over the Mojave desert (colors same as for a) except for 150 nm which is shown in purple). The residuals are the difference between observations and model calculations.

In Fig. 5a we show the surface polarized reflectance estimated from low altitude (150 m) measurements over the Dismal Swamp in Virginia together with the differences in surface polarized reflectance between the longest wavelength band (2250 nm) and the shorter wavelength bands. It can be seen that the surface polarized reflectance is indeed grey for this vegetated surface to within 10^{-4} in polarized reflectance units. Unfortunately we have no measurements of the surface polarized reflectance over deserts and so in Fig. 5b we show the observed polarized reflectance over the Mojave desert and the residual difference between the observations and model calculations that use the longest wavelength polarized reflectance as a proxy for the surface. The model calculations use AERONET observations¹² from Roger's Dry Lake as the basis for estimating an aerosol microphysical model and loading and a vector doubling/adding radiative transfer model to simulate the polarized reflectance of the atmosphere (in fact the upwelling at an altitude of 3500 m above the ground). The difference between model and measurements therefore includes uncertainties from the AERONET radiances, from the estimate of the aerosol model, from the calibration of the RSP radiances, from any errors in the model assumptions (grey polarized reflectance of the surface) and from any errors in the assumed geometry of the plane, which was coming in to land as this data was taken. The only conclusion we can draw from Fig. 5b is therefore that over the spectral range from 2250 to 412 nm there is little change (< 0.005) in the surface polarized reflectance. We also note that the optical depth on the day from which the data shown in Fig. 5b was taken (27th June 2002) was 0.085 at a reference wavelength of 550 nm. Thus, if the residual differences between model and measurements are a result of the surface polarized reflectance not being grey the effects of this error will be substantially less for the day on which we took data over smoke, since there was a substantially larger optical depth (< 1) on that day which obscures the surface.

Having ascertained that assuming the surface polarized reflectance of the desert is grey is a reasonable assumption at least when the aerosol burden is large we now show the fit between observed polarized reflectances and model calculations (Fig. 6b) that is obtained by an iterative search for a best fit model. The aerosol model that provided this fit has an optical depth of 1.24, an effective radius of 0.114 μm , an effective variance of 0.29, an imaginary refractive index of 0.07 and real refractive indices of 1.70131, 1.71513, 1.73128 and 1.76208 at 412, 469, 555 and 673 nm. The retrieved imaginary refractive index corresponds to a single scattering albedo of 0.77 at 550 nm which is similar to that (0.8) found for some African biomass burning³¹. The real refractive index is also retrieved at 863 nm but we do not report its value here because it is highly uncertain (± 0.15). The reason for this is that the effective radius is so small that at wavelengths longer than 700 nm the particles appear to be like Rayleigh scatterers and there is little sensitivity of the observed polarized reflectances to the refractive index of the particles. Although the real refractive index of the particles is quite high compared to other estimates^{31,32} the Mojave desert is an extremely dry environment which may cause the particles to be drier than typically observed. Also the peculiar feature of the observed polarized reflectances (increasing in absolute magnitude with increasing wavelength up to 863 nm then decreasing at 1590 nm) which is ubiquitous in our observations of smoke over a wide range of optical depths is difficult to explain without such a large real refractive index.

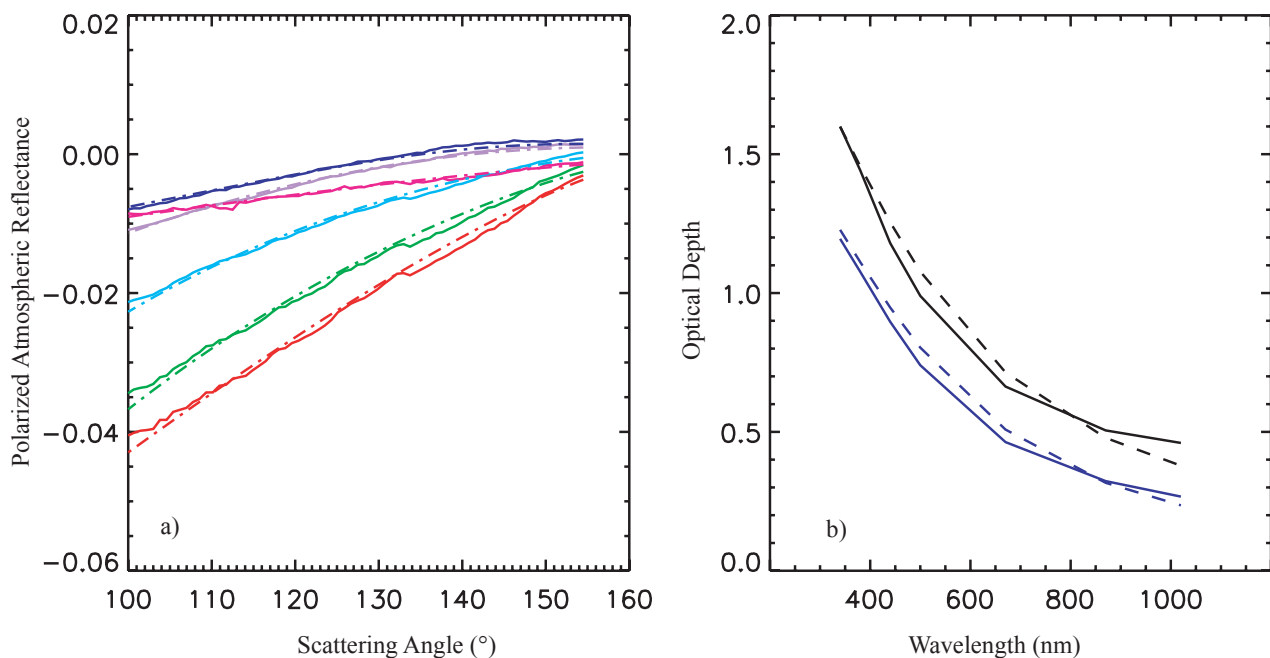


Fig. 6 a) Fit between model calculations of the atmospheric polarized reflectance (dot-dashed line) and observations corrected for surface contribution (solid line). Spectral bands are same as for Fig. 5. b) Comparison of spectral optical depths measured by AERONET (solid lines) before and after the RSP observations shown in a). Dashed lines show the microphysical model derived from the RSP measurements with the loading determined by fitting to the AERONET optical depth observations.

On the 29th October 2003 the aerosol load was highly variable and there was some patchy cirrus cloud cover present. Nonetheless the spectral variation of optical depth derived from the RSP retrievals that is shown in Fig 6b is consistent with that observed by AERONET. The two AERONET measurements shown in Fig. 6 were taken 15 minutes apart and are classified as cloud contaminated, although large variations in the smoke optical depth probably dominated over the cirrus contamination. We therefore conclude that the aerosol size retrieval from the RSP data is consistent with the AERONET observations but that cirrus cloud contamination and heterogeneity of the aerosol load mean that it is not possible to validate the aerosol optical depth estimate.

7. CONCLUSIONS

In this paper we have presented aerosol retrievals over ocean and land and retrievals of cloud properties for both ice and water clouds. Where good validation data is available the expected accuracy of the retrievals has been confirmed. Based on the analysis of this experimental data we expect the APS sensor to provide unprecedentedly accurate estimates of the load, type and composition of aerosols and of the size distribution, height and optical depth of water and ice clouds.

8. ACKNOWLEDGEMENTS

We would like to thank the NASA Radiation Sciences Program for support of our participation in CLAMS and in CRYSTAL-FACE through NAG5-11530, Dr. Steve Mango of the Independent Program Office and Professor John Seinfeld of California Institute of Technology for facilitating our participation in CSTRIFE and the NASA Glory project for supporting the acquisition of smoke data. The AERONET data used in this paper comes from an instrument that is mentored by Jeannette van den Bosch to whom we express our thanks for maintaining this site.

9. REFERENCES

- 1 Hansen, J. E., and Co-authors, 1998: Climate forcings in the industrial era, *Proc. Natl. Acac. Sci. USA*, **95**, 12,753–12,758.
- 2 Stamnes, K., W. Li, B. Yan, H. Eide, A. Barnard, W. S. Pegau, and J. J. Stamnes, 2003: Accurate and self-consistent ocean color algorithm: simultaneous retrieval of aerosol optical properties and chlorophyll concentrations, *Appl. Opt.*, **42**, 939–951.
- 3 Mishchenko, M. I., and Coauthors, 2004: Monitoring of aerosol forcing of climate from space: Analysis of measurement requirements, *J. Quant. Spectrosc. Radiat. Transfer* **88**, 149–161, doi:10.1016/j.jqsrt.2004.03.030.
- 4 Singer, J., 2002: Aerosol sensors on new weather satellites will improve forecasts, *SpaceNews*, August 12, p. 8.
- 5 Chowdhary, J., B. Cairns, M. Mishchenko, and L. Travis, 2001: Retrieval of aerosol properties over the ocean using multispectral and multiangle photopolarimetric measurements from the Research Scanning Polarimeter, *Geophys. Res. Lett.* **28**, 243–246, doi:10.1029/2000GL011783.
- 6 Cairns, B., L. D. Travis, and E. E. Russel, 1999: The Research Scanning Polarimeter: Calibration and ground-based measurements, *Polarization: Measurements, Analysis, and Remote Sensing*, D. H. Goldstein and D. B. Chenault, Eds., *Proc. SPIE*, **3745**, 186–196.
- 7 Barnes, R. A., R. E. Eplee, Jr., F. S. Patt, and C. R. McClain, 1999: Changes in the radiometric sensitivity of SeaWiFS determined from lunar and solar-based measurements, *Appl. Opt.*, **38**, 4649–4664.
- 8 Russell, E. E., and B. Cairns, 2002: Calibration system for calibration of various types of polarimeters, U.S. Provisional Application Ser. No. 60/363,308.
- 9 Redemann, J., and Co-authors, 2004: Suborbital measurements of spectral aerosol optical depth and its variability at sub-satellite grid scales in support of CLAMS, *J. Atmos. Sci.*, **62**, 1093–1117.
- 10 Magi, B. I., and Co-authors: Aerosol and chemical apportionment of aerosol optical depth at locations off the United States East coast in July and August 2001, *J. Atmos. Sci.*, **62**, 993–1007.
- 11 Jin, Z., and Coauthors, 2004: Radiation measurement and model simulation for the CLAMS experiment, *J. Atmos. Sci.*, **62**, 1093–1117.
- 12 Holben, B. N., and Co-authors, 1998: AERONET — A federated instrument network and data archive for aerosol characterization, *Remote Sens. Environ.*, **66**, 1–16.
- 13 Gordon, H. R., 1997: Atmospheric correction of ocean color imaginary in the Earth Observing System era, *J. Geophys. Res.*, **102**, 17 081–17 106.
- 14 Geogdzhayev, I. V., M. I. Mishchenko, W. B. Rossow, B. Cairns, and A. A. Lacis, 2002: Global two-channel aerosol AVHRR retrievals of aerosol properties over the ocean for the period of NOAA-9 observations and preliminary retrievals using NOAA-7 and NOAA-11 data, *J. Atm. Sci.*, **59**, 262–278.
- 15 Chowdhary, J., B. Cairns, and L. D. Travis, 2005: The contribution of waterleaving radiances to multiangle, multispectral photopolarimetric remote sensing observations over the open ocean: Bio-optical model results for case I waters, submitted to *J. Quant. Spectrosc. Radiat. Transfer*.

- 16 Chowdhary, J., and Co-authors, 2005: Retrieval of aerosol scattering and absorption properties from photopolarimetric observations over the ocean during the CLAMS experiment, *J. Atmos. Sci.*, **62**, 1093–1117.
- 17 Fridlind, A. M., and Co-authors, 2004: Evidence for the predominance of mid-tropospheric aerosols as subtropical anvil cloud nuclei, *Science*, **304**, 718–722.
- 18 Rolland, K. N. Liou, M. D. King, S. C. Tsay and G. M. McFarquhar, 2000: Remote sensing of optical and microphysical properties of cirrus clouds using the Moderate Resolution Imaging Spectroradiometer channels:
- 19 Garrett, T. J., H. Gerber, D. G. Baumgardner, C. H. Twohy and E. M. Weinstock, 2003: Small highly reflective ice crystals in low-latitude cirrus, *Geophys. Res. Lett.*, **30**, 2132–2135.
- 20 Liu, L., M. I. Mishchenko, B. Cairns, B. E. Carlson and L. D. Travis, Modeling single-scattering properties of cirrus by use of a size-shape distribution of ice spheroids and cylinders, to appear in *J. Quant. Spectrosc. and Radiat. Transfer*, 2005.
- 21 Macke, A., M. I. Mishchenko and B. Cairns, 1996: The influence of inclusions on light scattering by large ice particles, *J. Geophys. Res.*, **101**, 23,311–23,316.
- 22 C.-Labonnote, L., G. Brogniez, J.-C. Buriez and M. Doutriaux-Boucher, 2001: Polarized light scattering by inhomogeneous hexagonal mono-crystals: Validation with ADEOS-POLDER measurements, *J. Geophys. Res.*, **106**, 12,139–12,153.
- 23 Nakajima T., and M. D. King, 1990: Determination of the Optical Thickness and Effective Particle Radius of Clouds from Reflected Solar Radiation Measurements. Part I: Theory, *J. Atmos. Sci.*, **47**, 1878–1893.
- 24 Minnis, P., K.-N. Liou, and Y. Takano, 1993: Inference of cirrus cloud properties using satellite-observed visible and infrared radiances. I. Parameterization of radiance fields, *J. Atmos. Sci.*, **50**, 1279–1304.
- 25 Goloub, P., J. L. Deuzé, M. Herman, Y. Fouquart, 1994: Analysis of the POLDER polarization measurements performed over cloud covers, *IEEE Trans. Geosci. Rem. Sens.*, **32**, 78–88.
- 26 Mayer B., M. Schroder, R. Preusker, L. Schuller, 2004, *Atmos. Chem. Phys.*, **4**, 1255–1263.
- 27 Platnick, S., 2000: Vertical photon transport in cloud remote sensing problems, *J. Geophys. Res.*, **105**, 22,919–22,935.
- 28 Mishchenko M. I., L. D. Travis, W. B. Rossow, B. Cairns, B. E. Carlson, and Q. Han Q, 1997: Retrieving CCN column density from single-scattering measurements of reflected sunlight over the ocean: A sensitivity study, *Geophys. Res. Lett.* **24**, 2655–2658.
- 29 Hudson, J., and S. S. Yum, 1997: Droplet spectral broadening in marine stratus, *J. Atmos. Sci.*, **54**, 2642–2654
- 30 Khvorostyanov, V. I., and J. A. Curry, 1999: Toward the Theory of Stochastic Condensation in Clouds. Part II: Analytical Solutions of the Gamma-Distribution Type, *J. Atmos. Sci.*, **56**, 3997–4013.
- 31 Kreidenweis, S. M., L. A. Remer, R. Bruintjes and O. Dubovik, 2001: Smoke aerosol from biomass burning in Mexico: Hygroscopic smoke optical model, *J. Geophys. Res.*, **106**, 4831–4844.
- 32 Yamasoe, M. A., Y. J. Kaufman, O. Dubovik, L. A. Remer, B. N. Holben and P. Artaxo, 1998: Retrieval of the real part of the refractive index of smoke particles from Sun/sky measurements during SCAR-B, *J. Geophys. Res.*, **103**, 31,893–31,902.